Actuator Fault Monitoring and Fault Tolerant Control in Distillation Columns

S A Lawal[1,2]   J Zhang[1]

[1]School of Chemical Engineering and Advanced Materials, Newcastle University, Newcastle upon Tyne, NE1 7RU, UK

[2] Department of Chemical Engineering, University of Lagos, Akoka, Yaba, Lagos, Nigeria

Abstract: This paper presents, from a practical viewpoint, an investigation of real-time actuator fault detection, propagation and accommodation in distillation columns. Addressing faults in industrial processes, coupled with the growing demand for higher performance, improved safety and reliability necessitates implementation of less complex alternative control strategies in the events of malfunctions in actuators, sensors and or other system components. This work demonstrates frugality in the design and implementation of fault tolerant control system by integrating fault detection and diagnosis techniques with simple active restructurable feedback controllers and with backup feedback signals and switchable reference points to accommodate actuator fault in distillation columns based on *a priori* assessed control structures. A multivariate statistical process monitoring based fault detection and diagnosis technique through dynamic principal components analysis is integrated with one-point control or alternative control structure for prompt and effective fault detection, isolation and accommodation. The work also investigates effects of disturbances on fault propagation and detection. Specifically, the reflux and vapor boil-up control strategy used for a binary distillation column during normal operation is switched to one point control of the more valued product by utilizing the remaining healthy actuator. The proposed approach was implemented on two distillation processes - a simulated methanol-water separation column and the benchmark Shell standard heavy oil fractionation process to assess its effectiveness.

Keywords: Dynamic principal component analysis, fault detection and diagnosis, distillation column, fault tolerant controller, inferential control.

1   Introduction

Application of fault tolerant control systems (FTCS) in industrial processes offers high performance, improved safety, reliability and availability in the presence of faults in sensors, actuators and some other system components. FTCS is a closed-loop control system with automatic components containment capabilities and provides desirable performance on complex automated facilities whether faults are present or not. A requirement for the design of an FTCS is an effective fault detection and diagnosis (FDD) system to detect faults and provide information on their locations and magnitudes. Early detection of faults and availability of reliable information on process upsets, equipment malfunctions and presence of any unusual events in a system is very important, so as to maintain such system within its desired operating region. Billions of dollars are lost in the industry every year due to low productivity, loss of operational hours, occupational injuries and illnesses resulting from major and common minor accidents occurring on a daily basis [1−3]. It is inevitable that some processing equipment including actuators, sensors and control systems will breakdown or malfunction at some point during their operational life span. So, it will be desirable to have FTCS that are able to accommodate those potential failures during operation while still maintaining acceptable level of performance, albeit with some graceful degradation. Implementation

of frugally designed FTCS that is able to perform the function of a much more complex FTCS will be a welcome development, especially to the plant operators who favor less complex control systems.

FDD is a crucial component of an FTCS. Its effectiveness will to a large extent determine the applicability, effectiveness and overall functionality of the resulting FTCS. As it is the case with the conventional control systems, an understanding of the faulty actuators and their effects would be required in either a mathematical or statistical form to enable the design of suitable FTCS for the controlled process. Researches into FDD as an integral part of an FTCS span over four decades with wide spectrum of techniques developed in different application areas. Some of the techniques used in FDD design are quantitative model-based [4,5] where models developed from first principles are used; qualitative model-based [6,7] where understanding of failures and symptoms are modeled for fault detection and diagnosis; and data-based/process history-based approach [8−14] where past and current measurements of the process are used for FDD. The difficulties faced in developing detailed first principle models for complex chemical processes with acceptable level of accuracy needed for fault monitoring and accommodation purposes limit the application of the model-based FDD to well understood systems like electro-mechanical systems. Data-based FDD on the other hand has been extensively used in the chemical industries for process monitoring and fault diagnosis because of its ability to provide reduced dimensional models for high dimensional processes. Its wide usage also stems from its simplicity and ability to handle large amount of correlated process measurements. Hence

the focus of this paper is on data-based FDD using dynamic principal component analysis (DPCA). A brief description of how DPCA is applied for FDD is presented in Section 2. Readers interested in other approaches should consult references [4,6,8,9].

Reconfigurable or restructurable controller (RC) also known as fault tolerant controller (FTC) is an integral part of fault tolerant control system. Its main objective is to accommodate faults when one is deemed to have occurred so as to maintain the system within an acceptable operating region. FTC is a sophisticated control system with capabilities well beyond the reach of conventional control system. They are capable of tolerating failures or malfunctions in system components, actuators and sensors and still deliver satisfactory performance despite those failures. Several techniques have been used in the design of FTC over the last three decades. Reference [15] gave a detailed classification of such techniques. Some of the interesting results on the design and application of FTC that have been published lately include application of distributed model predictive control (DMPC) to accommodate actuator faults in a three unit continuous stirred tank reactor [16,17]; combined use of model predictive control (MPC) and H_∞ robust controller [18]; the use of proactive fault tolerant Lyapunov-based MPC [19] and the use of three different principal component analysis (PCA) based techniques, multi-block PCA (MPCA) and DPCA integrated with MPC in monitoring, analysis, diagnosis and control with agent-based systems for FDD and FTC [20]. One common feature of all these techniques is the high level of complexity and computational task involved in their design and implementation. A simple restructurable feedback controller like PID with backup feedback signals and switchable reference points may be able to achieve the same result with much less effort, though different possible control structures would have to be analyzed *a priori* using tools like relative gain array (RGA) and relative disturbance gain analysis to select possible switching options. As it is often the case that, for any given process, there are several ways of controlling it, some better than others, so selecting a sub-optimal strategy under faulty condition would be far more acceptable than process shut-down. However, the switchability and restructurability of a fault tolerant controller is process dependent as maintaining acceptable level of performance in some processes may not always be achievable due to lack of suitable controlled and manipulated variable pairing. This has to be carefully assessed taking into consideration the remaining healthy actuators and the process variables pairing for control purposes. This paper explores the option of applying fault tolerant PID controller philosophy to some common processes in the chemical industry.

Distillation column is among the most common and energy intensive plant units. The dynamics and control of distillation column has been extensively studied because of its fundamental importance to the chemical and process industries [21−27]. However, from practical viewpoint and to the best of our knowledge, application of simple conventional PID controller with extended restructurable capability to the operation and control of distillation processes under faulty components such as actuators

and sensors have not been widely reported. Owing to its importance in the process industries, this paper focuses on the implementation of simple conventional PID controllers with extended restructurable capability to accommodate actuator faults in a comprehensive nonlinear methanol-water separation column and the benchmark Shell standard control problem which is a highly constrained 5 inputs 7 outputs heavy oil fractionator.

This paper is an extension of our previous work [28], it presents a two-stage fault tolerant control system for a binary distillation column and a heavy oil fractionator. First, the presence of fault is detected using DPCA which incorporates time-lagged process variables to properly capture the system dynamics and its effect on actuator fault propagation. Upon detection of a fault, contribution plots are used to diagnose the fault. The second stage involves restructuring the control configuration to accommodate the detected faults. If the fault is an actuator fault, in the case of a binary distillation column then two-point control strategy cannot be functional and has to be switched to one-point control. The most valued product composition is then controlled directly using the remaining healthy actuator to limit the impact of actuator fault. If the detected fault in the binary distillation column is a composition sensor fault, then composition sensor feedback control involving the faulty composition sensor will not be functional and inferential control by-passing the faulty sensor can be implemented.

The structure of the paper is as follows. Section 2 discusses FDD, DPCA and the proposed FTC while Section 3 presents application of the proposed FTC to methanol-water separation column. Investigation of the Shell heavy oil fractionator under FTC is presented in Section 4 and Section 5 gives some concluding remarks.

2 DPCA and FTC Strategy

2.1 DPCA

DPCA is the dynamic variant of PCA, a static multivariate statistical projection technique that is based on orthogonal decomposition of the covariance matrix of the process variables along direction that explains the maximum variation of the data. DPCA finds factors that have a much lower dimension than the original data set and can properly describe the major trend in the original data set. It incorporates time-lagged measurements in its model to capture the dynamic correlation behavior of the system for effective fault propagation analysis. DPCA method can be briefly summarized as follows: let X be an $n \times (l+1)p$ matrix of the scaled measurements of n samples and p variables with covariance matrix Σ where l is the number of time lags considered. From matrix algebra, Σ may be reduced to a diagonal matrix L by a particular orthonormal $(l+1)p \times (l+1)p$ matrix U, i.e.

$$\Sigma = ULU^T \qquad (1)$$

where columns of U are the principal component (PC) loading vectors and the diagonal elements of L are the ordered eigenvalues of Σ which defines the amount of variance explained by the corresponding eigenvector. Then,

the dynamic principal component transformation is given as:

$$T = XU \quad or \quad t_i = Xu_i \tag{2}$$

Equivalently, X is decomposed by PCA as:

$$X = TU^T = \sum_{i=1}^{(l+1)p} t_i u_i^{'} \tag{3}$$

The $n \times (l+1)p$ matrix $T = (t_1, t_2, ..., t_{(l+1)p})$ contains the so-called *principal component scores* which are linear combinations of all $(l+1)p$ variables. Generally, the first few PCs will capture the most variation in the original data if the variables are correlated. Typically the first "a" principal components ($a < (l+1)p$) can be used to represent the majority of data variation:

$$X = t_1 u_1^{'} + ... + t_a u_a^{'} + E = \sum_{i=1}^{a} t_i u_i^{'} + E \tag{4}$$

where E is the resulting residual term due to ignoring the rest of the principal components. Hotelling's T^2 and the squared prediction error (SPE) monitoring statistics given below are used to detect fault from new measurements.

$$T_i^2 = \sum_{j=1}^{a} \frac{t_{i,j}^2}{\lambda_j} \tag{5}$$

where T_i^2 is the Hotelling's T^2 value for sample i, $t_{i,j}$ is the ith element of principal component j, λ_j is the eigenvalue corresponding to principal component j, and a is the number of principal components retained.

When the process is in normal operation, both SPE and T^2 should be small and within their control limits. When a fault appears in the monitored process, the fault will cause some variables having larger than normal magnitudes (large T^2 values) and/or change the variable correlations leading to large SPE values. The control limits for SPE and T^2 are given by (6) and (7) respectively.

$$
\begin{cases}
SPE = \theta_1 \left[\frac{c_\alpha h_0 \sqrt{2\theta_2}}{\theta_1} + 1 + \frac{\theta_2 h_0 (h_0 - 1)}{\theta_1^2} \right]^{\frac{1}{h_0}} \\
\\
\theta_i = \sum_{j=a+1}^{p} \lambda_j^i \\
\\
h_0 = 1 - \frac{2\theta_1 \theta_2}{3\theta_2}
\end{cases}
\tag{6}
$$

$$T_{lim}^2 = \frac{a(n-1)}{(n-a)} F_{a,n-a,\alpha} \tag{7}$$

In (6) and (7), c_α is the value for normal distribution at $100(1 - \alpha)\%$ confidence level and $F_{a,n-a,\alpha}$ is the F distribution with appropriate degrees of freedom and confidence level.

2.2 FTC Strategy

An insight into the design of conventional PID controller with extended restructurable capability for FTC is presented in this section. PID controllers are relatively easy to implement and are popular among plant operators. An extended version of the controller with restructurable capabilities to accommodate actuator and sensor faults

without any doubt will be a good addition to the list of growing FTCs for industrial applications. The structure of the proposed fault tolerant PID controller is presented in Fig. 1. The dashed lines in Fig. 1 indicate controller switching in the event of a fault being detected and diagnosed. The structure is an extension of the standard feedback control with integrated switchable reference points (set points) to allow for switching of set points; FDD scheme to detect and identify possible occurrence of faults; restructurable PID controllers for actuator fault accommodation and soft sensor estimator for controlled variables (primary outputs) estimation from secondary measurable process variables to accommodate possible sensor faults. The major difference between the standard feedback control loop and the proposed FTC strategy is the integration of controlled variables' backup feedback signals (y_b) and their estimates (y_{est}), backup manipulated variables (u_b) and the set points signals (r_s). u_c and d are controller outputs and disturbances respectively. The solid feedback signals are used for control purposes during normal operation while the dashed lines represent back-up feedback signals for implementation of the proposed FTC. Given the control error generated for a conventional feedback control law as:

$$e = r - y_p \tag{8}$$

and with backup feedback signal for an actuator fault as:

$$e = r_r - y_p \tag{9}$$

where

$$r_r = [r^T \quad r_s^T]^T \quad and \quad y_y = [y_p^T \quad y_b^T]^T \tag{10}$$

In the equations and in Fig. 1, e, r, r_s, y_p, and y_b, are vectors of appropriate dimensions for the error signal, set points, switchable set points for backup feedback signal, controlled outputs and their backup feedback signals respectively. To accommodate sensor fault, y_p in (10) will be replaced by soft sensor estimate y_{est} in place of the faulty sensor outputs. Sensor fault accommodation is not considered in this work. Weighting matrices are introduced into (9) for the purpose of restructuring the FTC and it is presented in a more compact form as:

$$e = \beta_r r_r - \beta_y y_y \tag{11}$$

where

$$
\begin{cases}
\beta_r = diag(\beta, \quad \beta_s) = \begin{bmatrix} \beta & 0 \\ 0 & \beta_s \end{bmatrix} \\
\\
\beta_y = diag(\beta_p, \quad \beta_b) = \begin{bmatrix} \beta_p & 0 \\ 0 & \beta_b \end{bmatrix}
\end{cases}
\tag{12}
$$

β, β_s, β_p, and β_b are square weighting matrices of appropriate dimensions for set points, set point backup signal, controlled outputs and the controlled outputs backup feedback signals respectively. During normal operation, β and β_p are identity matrices while β_s and β_b are zero matrices. The weightings are used to deactivate and activate actual and backup feedback signals as appropriate during fault tolerant controller reconfiguration. Given the reconfigurable PID controllers as:
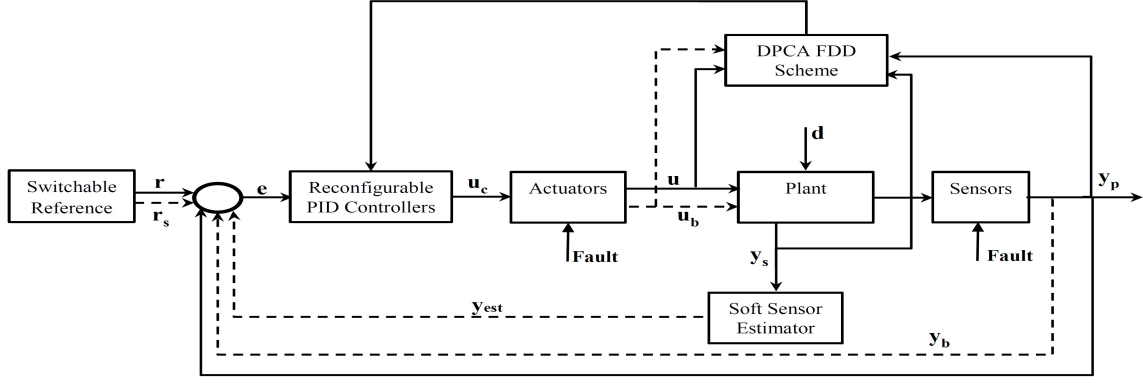
Fig. 1   Fault Tolerant PID Controllers with Backup Feedback Signals.

$$G_R = [G_c^T \quad G_b^T]^T \tag{13}$$

where G_c and G_b are the actual controllers used during normal process operation and pre-assessed backup controllers to accommodate possible fault occurrence, respectively. To implement the reconfigurable controllers, another weighting matrix β_R is introduced in (13) which now becomes:

$$G_{RC} = \beta_R G_R \tag{14}$$

The control law for the reconfigurable fault tolerant PID controller G_{RC} is then given as:

$$u = G_{RC} e \tag{15}$$

The different possible manipulated and controlled variable pairings are assessed *a priori* to decide on the reconfiguration pairing upon detection and identification of a fault. Hence, accommodation of any individual fault is dependent on having a suitable healthy actuator that is able to provide satisfactory performance in the impaired system. Only a single fault tolerant control system is considered in this work, however the approach can also be applied to duplex FTCS structure. By single and duplex FTCS, we mean a single and double fault tolerant control system backup for each pre-assessed fault provided there are suitable restructurable manipulated and controlled variables pairings. The proposed FTCS is applied to two systems, a simulated methanol-water distillation column and the benchmark Shell heavy oil fractionator to assess its efficacy.

3 Application to methanol water separation column

3.1 System description

The distillation column studied in this paper is a comprehensive nonlinear simulation of a methanol-water separation column. A nonlinear stage-by-stage dynamic model has been developed using mass and energy balances. The simulation has been validated against pilot plant test and is well known for its use in control system performance

studies [20−22]. The following assumptions are imposed on the column model: negligible vapor hold-up, perfect mixing in each stage, and constant liquid hold-up. Table 1 presents the steady-state conditions for the column.

The column was simulated in MATLAB with 30 seconds sampling time using the LV control strategy. The top composition (Y_D) is controlled by the reflux flow rate (L) and the bottom composition (X_B) by the steam flow rate (V) to the reboiler. Levels in the condenser and the reboiler are controlled by the top and bottom flow rates respectively. The disturbances in the system are feed flow rate and feed compositions. The top and bottom product compositions are measured by composition analyzers with 10 sampling times delay (5 minutes).

Table 1   Nominal column operating data

Column Parameters	Values
No of theoretical stages	10
Feed tray	5
Feed composition (Z)	50% methanol
Feed flowrate (F)	18.23 g/s
Top composition (Y_D)	0.95 (weight frac.)
Bottom composition (X_B)	0.05 (weight frac.)
Top product flow rate (D)	9.13 g/s
Bottom product flow rate (B)	9.1 g/s
Reflux flow rate (L)	10.11 g/s
Steam flow rate (V)	13.81 g/s

3.2 Fault introduction and detection

Low and high magnitude faults were introduced into the system at different times by restricting the flow of reflux and steam rates to represent stuck valves, thereby acting as actuator faults as shown in Table 2. Four low magnitude actuator faults (F1, F3, F6, and F7) were investigated, with values of the manipulated variables held close to their respective steady state values. The first 2 low magnitude faults (F1 and F3) are investigated for low magnitude fault detectability while the last 2 low magnitude faults (F6 and F7) were introduced to investigate effects of disturbances on low magnitude faults propagation and detectability. Also, two high magnitude actuator faults (F2 and F4) and a combination of the two high magnitude actuator faults (F5)

Table 2   Distillation column fault list

Fault	Fault description
F1	Reflux valve stuck btw 7-10 g/s after sample 750
F2	Reflux valve stuck btw 5- 8 g/s after sample 750
F3	Steam valve stuck btw 10-14 g/s after sample 750
F4	Steam valve stuck btw 10-13 g/s after sample 750
F5	Reflux and steam valves stuck @ 8 g/s and 13 g/s after samples 750 and 1150 respectively
F6	F1 repeated with feed flow rate disturbance introduced after sample 900
F7	F3 repeated with feed flow rate disturbance introduced after sample 900
F8	Top composition sensor fault with sensor value set at 0.75 after sample 750 (static)
F9	Bottom composition sensor fault with sensor value set at 0.03 after sample 750 (static)

are considered. Similarly, two sensor faults, top composition (F8) and bottom composition (F9) sensor faults, were investigated to assess the ability of the DPCA FDD technique to diagnose different faults using contribution plots. The fault cases were each simulated for 750 minutes to collect 1500 samples.

There were a total of 14 monitored variables: the top and bottom product compositions, the manipulated variables – reflux and steam flows, and the ten tray temperatures. Random noises with zero means and 0.15 and 0.001 standard deviations were added to the ten tray temperatures and the top and bottom compositions respectively, to represent true measurements of the data collected. Fig. 2 presents the top and bottom compositions, their respective manipulated variables and the ten tray temperatures for normal operating conditions.
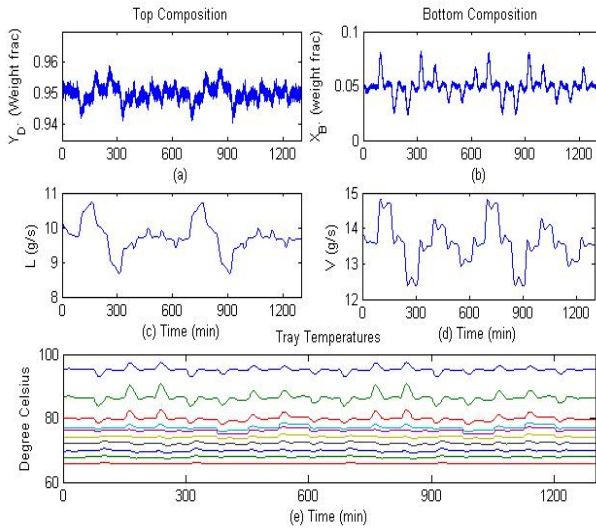

Fig. 2   (a) Top composition; (b) Bottom composition; (c) Reflux flow rate; (d) Steam flow rate; (e) Tray temperatures.

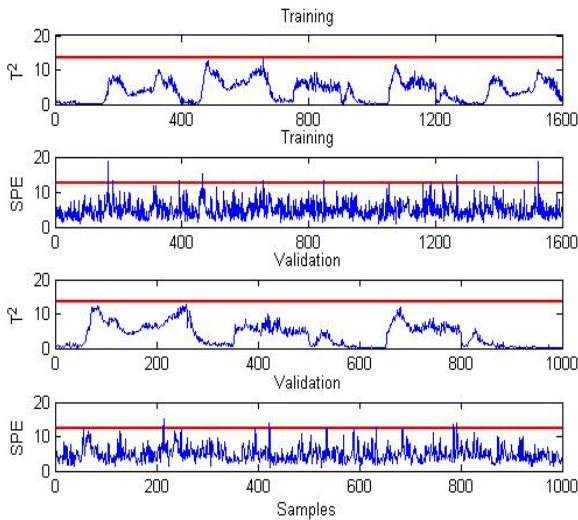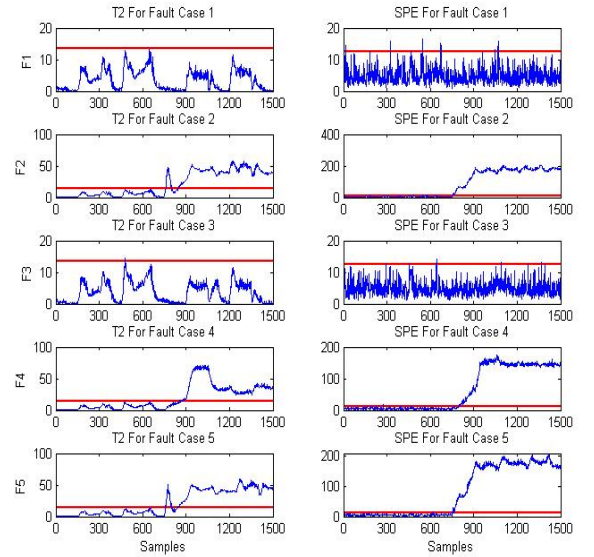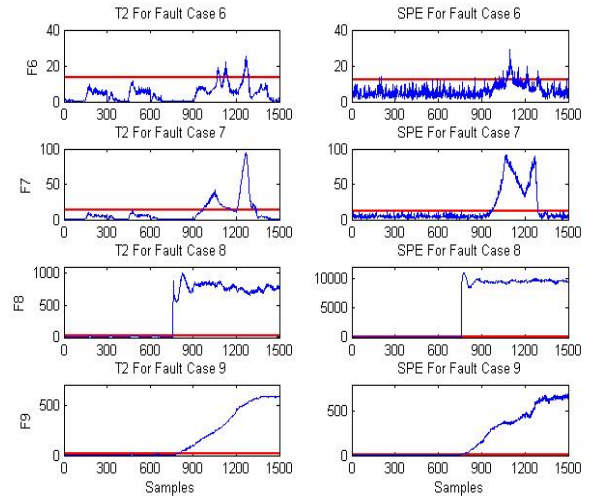Fig. 4 T^2 and SPE plots for fault cases F1 to F5.

Fig. 3   DPCA monitoring performance.

Fig. 5 T^2 and SPE plots for fault cases F6 to F9.

A DPCA model was developed using the first 1600 samples out of the 2600 collected under normal conditions while the last 1000 samples were used for validation. The data was scaled to zero mean and unit variance.

Four principal components account for 82.17% variations in the original data and are sufficient to develop the DPCA diagnostic model. The developed DPCA diagnostic model for the fault free system is applied to the nine faulty data sets to detect faults. Fig. 3 presents the T^2 and SPE monitoring plots for the fault-free system while Figs. 4 and 5 show those of the nine fault cases (F1 – F9). A fault is declared after the control limits are violated for four successive sampling times to reduce occurrence of false alarms. Once the presence of a fault is detected, further fault identification analysis is carried out through contribution plots to identify variables that are responsible for the faults, and ultimately isolate the faults. Figs. 6 and 7 present the contribution plots for the fault cases considered.
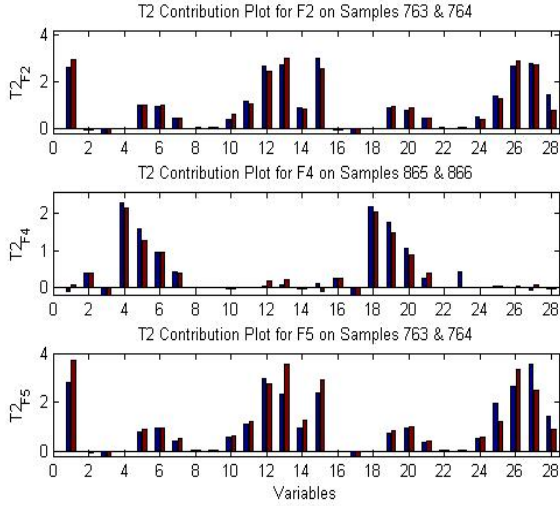

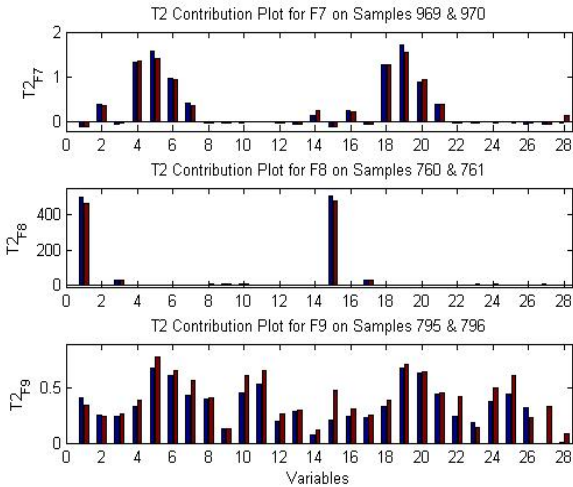Fig. 6 T^2 Contribution plots for F2, F4 and F5.

Fig. 7 T^2 Contribution plots for F7, F8 and F9.

3.3   Actuator fault accommodation

The proposed FTC strategy is applied to the distillation column upon detection of an actuator fault. The two actuators investigated in the system are reflux flow and steam flow actuators with varying degrees of faults as presented in Table 2. The error signals generated by the system during normal operation for the top and bottom composition controllers (G_c) is given by (11) as:

$$e = \begin{bmatrix} 1 & 0 & 0 & 0 \\ 0 & 1 & 0 & 0 \\ 0 & 0 & 0 & 0 \\ 0 & 0 & 0 & 0 \end{bmatrix} \begin{bmatrix} r_1 \\ r_2 \\ r_{s1} \\ r_{s2} \end{bmatrix} - \begin{bmatrix} 1 & 0 & 0 & 0 \\ 0 & 1 & 0 & 0 \\ 0 & 0 & 0 & 0 \\ 0 & 0 & 0 & 0 \end{bmatrix} \begin{bmatrix} y_1 \\ y_2 \\ y_{b1} \\ y_{b2} \end{bmatrix} \tag{16}$$

It can be observed that the backup signals are zeros as their weightings are zeros. When an actuator fault is detected and subsequently identified, say for instance, the reflux flow actuator, the reconfigurable controller is then activated using the other healthy actuator, in this case steam valve actuator, provided the top composition is deemed more valuable. Equation (16) then becomes:

$$e = \begin{bmatrix} 0 & 0 & 0 & 0 \\ 0 & 0 & 0 & 0 \\ 0 & 0 & 1 & 0 \\ 0 & 0 & 0 & 0 \end{bmatrix} \begin{bmatrix} r_1 \\ r_2 \\ r_{s1} \\ r_{s2} \end{bmatrix} - \begin{bmatrix} 0 & 0 & 0 & 0 \\ 0 & 0 & 0 & 0 \\ 0 & 0 & 1 & 0 \\ 0 & 0 & 0 & 0 \end{bmatrix} \begin{bmatrix} y_1 \\ y_2 \\ y_{b1} \\ y_{b2} \end{bmatrix} \tag{17}$$

and the control law for accommodating the reflux valve actuator fault is obtained using (15) as:

$$u = \begin{bmatrix} u_1 \\ u_2 \\ u_{b1} \\ u_{b2} \end{bmatrix} = \begin{bmatrix} 0 \\ 0 \\ G_{b1} \\ 0 \end{bmatrix} \begin{bmatrix} 0 \\ 0 \\ r_{s1} - y_{b1} \\ 0 \end{bmatrix} \tag{18}$$

Equation (18) presents the reconfigured controller that accommodates reflux valve actuator fault using steam valve actuator while the bottom composition is left uncontrolled. The procedure is the same if the steam valve actuator fault is declared.

3.4   Simulation results

Figs. 4 and 5 show the T^2 and SPE plots for faults F1 to F5 and F6 to F9 respectively. Fig. 6 shows the contribution plots for F2, F4 and F5 while Fig. 7 presents those of F7, F8 and F9. Figs. 6 and 7 present the excess contributions of each variable to the larger than normal value of T^2 at the point of fault declaration. By excess contributions, we mean the difference between contributions of each variable to the values of T^2 at the point of fault declaration and their respective average contribution under fault free conditions. From the analysis of T^2 and SPE plots shown in Figs. 4 and 5, the monitoring statistics for faults F2, F4, F5, F7, F8 and F9 exceeded their control limit at different times during the simulation so these faults were detected. Faults F2 and F5 were detected 13 sampling times (6 mins 30 sec.) after introduction, on sample 763, while it took 115 sampling times (approximately 58 mins), on sample 865 for fault effect to manifest in F4 as presented

in Fig. 4. Fault 7 (F7) was detected on sample 969, approximately 110 minutes after it was introduced as shown in Fig. 5. Note that faults F3 and F7 are exactly the same with the exception of disturbances introduced after the faults to investigate the effects of the disturbances on the faults propagation and detectability. A 10% increase in feed composition disturbance was introduced at sample 900 in the case of F3 while the same magnitude of disturbance in feed flow rate was introduced in the case of F7, also at sample 900.

Basically, disturbances do affect fault propagation and detection in the column, and could amplify a rather minor undetected fault as shown in the case of F7 which was detected 69 sampling times (approx. 35 minutes) after the disturbance was introduced. Further analyses were conducted to identify the faults using contribution plots upon declaration of a fault. The T^2 contribution plots gave a more consistent indication of the variables responsible for the faults; hence only T^2 contribution plots are used for fault identification. In the case of F2 and F5 where reflux actuation faults were identified, the contribution plot as shown in Fig. 6 identified the top composition and the top four tray temperatures (variables 1, 11, 12, 13, 14, 25, 26, 27 and 28) as the major contributors to the out-of-control situation. Analysis of the T^2 contribution plots presented in Figs. 6 and 7 combined with the process knowledge aided the fault identification. For instance, when the reflux actuator fault occurred (stuck reflux valve), and after it has been detected, the contribution plot isolates variables indicative of the fault. The detected reflux actuator fault with reduced reflux flow caused the top tray temperature measurements to rise by certain percentage which ultimately led to the top composition drifting out of control. Hence, the contributions of these variables (top composition and the top tray temperatures) to the T^2 monitoring statistics increased significantly as presented in Fig. 6. The rise in the top tray temperature measurements as a consequence of reduced reflux flow is peculiar to the reflux actuation fault, which aided its isolation. Similarly, observing contribution plots for F4 and F7 as presented in Figs. 6 and 7; when steam actuator fault occurred the bottom composition drifted out of control which also affected the steam controller output and the bottom tray temperatures. These effects manifest in the larger than average contributions of these variables to the T^2 values at the point of fault declaration and beyond. This was the pattern exploited in the faults identifications as different faults show different variable contributions to the T^2 values after occurrence of a fault.

As mentioned in Table 2, F1, F2 and F6 are all reflux actuator faults of different magnitudes; while F3, F4 and F7 are steam actuator faults, also of different magnitudes. F5 is a combination of reflux and steam actuator faults, but with reflux actuator fault occurring first. Faults 8 and 9 (F8 and F9) are the top and bottom compositions sensor faults which were also detected and identified respectively. Contribution plot for the top composition sensor fault (F8) shows the top composition (the sensor output) as the only variable responsible for the fault while the bottom composition sensor fault (F9) indicates that all the variables are responsible for the fault as presented in Fig. 7.

Observations from Figs. 6 and 7 show different variable contribution patterns which aided fault isolation. Faults F1, F3 and F6 were not detected due to the fact that only small changes were made to the values of the two actuators which were close to the nominal values of the two manipulated variables as shown in Table 1 under reflux and steam flow rates. The resulting values for the process variables were within normal conditions. Fault 6 (F6), a rather minor undetected fault in F1, was affected by the amplifying effect of the disturbance (increased in feed flow rate after sample 900) on its propagation which moved it to marginal stability.

Clearly, the conventional LV control strategy used for the column normal operation could not accommodate the actuator faults. Hence, the control strategy in the column is restructured by switching to one-point control strategy where the only remaining healthy actuator, steam flow rate actuation in the case of F2 and F5 and reflux flow rate actuation in the case of F4 and F7 were used to accommodate the faults and maintain the more valuable outputs of the two compositions within acceptable range while the other is uncontrolled. Steam flow actuation was immediately restructured and implemented to tolerate reflux valve faults, F2 and F5 by manipulating the steam flow rate to directly maintain the top composition at its set point thereby tolerating reflux valve actuation faults in F2 and F5 as presented in Fig. 8.

Table 3   Distillation column controller settings

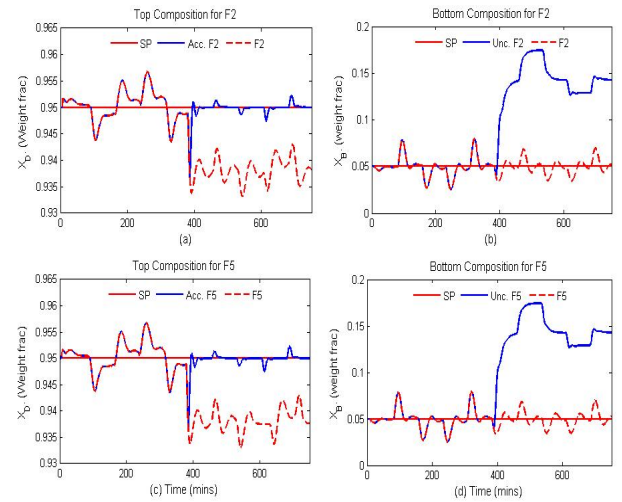| | Controller parameters | | | |
	PI loop 1		PI loop 2	
	K_{P1}	T_{I1}	K_{P2}	T_{I2}
Normal operation	45	18.67	-20	18.38
Reflux actuator fault acc.	–	–	-100.5	13.5
Steam actuator fault acc.	70.7	21	–	–

Fig. 8   Responses of the top and bottom composition to F2 and F5 reflux actuator faults accommodation.

Table 3 presents the reconfigurable PI controller settings for the column under normal and faulty conditions. Similarly, upon detection of steam flow actuation faults, F4 and F7,

the column control structure was immediately switched to reflux valve one-point control by manipulating reflux flow rate to directly maintain the bottom composition at set point if the bottom composition is deemed more important, thereby tolerating the steam flow actuation faults F4 and F7 as shown in Fig. 9. It is worth mentioning at this point that, the fault accommodation approach proposed in this work is sub-optimal as it is practically impossible to use one manipulated variable to maintain both top and bottom compositions at set points. The sub-optimal fault accommodation approach provides desirable performance and will be far more acceptable than shut-down. SP, Unc. and Acc. are used in Figs. 8 and 9 to represent set point, uncontrolled fault and accommodated fault respectively.

The effects of disturbances, feed flow rates and the feed compositions after the faults were well compensated for by the fault tolerating control approach as can be observed in Figs. 8 and 9. Sensor fault accommodation strategy is not investigated in this paper, and its detection and identification is only included in this work to demonstrate the effectiveness of DPCA based FDD approach.
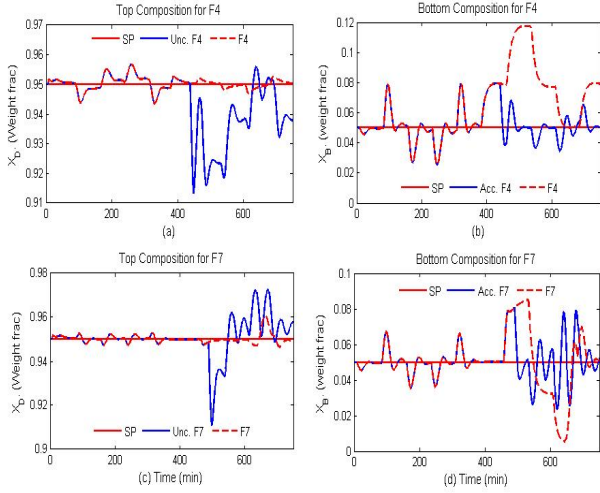

Fig. 9   Responses of the top and bottom composition to F4 and F7 steam actuator faults accommodation.

4 Application to Shell heavy oil fractionator

4.1 Shell heavy oil fractionator

The Shell heavy oil fractionator benchmark was developed by Shell Company as a test bed for the assessment of new control theories and technologies in 1986 [29,30]. It is a highly constrained multivariable process with very strong interactions amongst its control loops and large dead times. The original system is slightly modified in this study by relaxing some of its constraints for the purpose of actuator faults accommodation. The heavy oil fractionator has 5 inputs and 7 outputs, and it provides a realistic test bed for control related studies. The process was modelled using a first-order plus dead time transfer function matrix. Three out of the 5 inputs (top draw - u_1, side draw - u_2 and bottom reflux duty - u_3) into the system are used as manipulated variables, directly maintaining 3 process outputs (top end point - y_1,

side draw end point - y_2 and bottom reflux temperature - y_7) at their set points while the remaining 2 inputs serve as unmeasured disturbances into the system. The other 4 outputs are not controlled. Table 4 gives the full listing of all the system variables. The manipulated variables are subject to saturation (± 0.5) and rate limit (± 0.5 per sample time) actuator hard constraints, which introduce non-linearity into the system. The disturbances are bounded within absolute values not more than 0.5. The complete model of the system is given in the appendix while Fig. 10 presents the system with different back-up feedback signals (indicated by dashed lines) for possible implementation of actuator fault tolerant controller. The system is controlled using 3 reconfigurable PI controllers with integral anti-windup.

Table 4   Variables for the heavy oil fractionator

Variables	Output variables
Variable 1	Top end point (y_1)
Variable 2	Side end point (y_2)
Variable 3	Top temperature (y_3)
Variable 4	Upper reflux temperature (y_4)
Variable 5	Side draw temperature (y_5)
Variable 6	Inter. reflux temperature (y_6)
Variable 7	Bottom reflux temperature (y_7)
	Input variables
Variable 8	Top draw (u_1)
Variable 9	Side draw (u_2)
Variable 10	Bottom reflux duty (u_3)
	Disturbance variables
	Inter. reflux duty (d_1)
	Upper reflux duty (d_2)

The input – output selection for the control configuration was achieved after careful analysis of the system coupled with the use of relative gain array (RGA) analysis. The transfer function matrix of the system is given in (19) below. Equation (19) is used to obtain the steady state RGA for the system as shown in (20).

$$G(s) = \begin{bmatrix} \frac{4.05e^{-27}}{50s+1} & \frac{1.77e^{-28}}{60s+1} & \frac{5.88e^{-27}}{50s+1} \\ \frac{5.39e^{-18}}{50s+1} & \frac{5.72e^{-14}}{60s+1} & \frac{6.90e^{-15}}{40s+1} \\ \frac{4.38e^{-20}}{33s+1} & \frac{4.42e^{-22}}{44s+1} & \frac{7.20}{19s+1} \end{bmatrix} \quad (19)$$

$$RGA = \begin{bmatrix} 2.0757 & -0.7289 & -0.3468 \\ 3.4242 & 0.9343 & -3.3585 \\ -4.4999 & 0.7946 & 4.7053 \end{bmatrix} \quad (20)$$

Based on the RGA values, the manipulated variables u_1, u_2 and u_3 are used to control y_1, y_2 and y_7 respectively, producing a 3×3 control configuration. The heavy oil fractionator was simulated without actuator faults in Simulink for 2000 minutes with 1 minute sampling time to collect 2000 samples of the 7 outputs and 3 manipulated variables. Intermediate reflux duty (d_1) and upper reflux duty (d_2) serve as disturbances in the system and were randomly introduced into the fractionator during normal
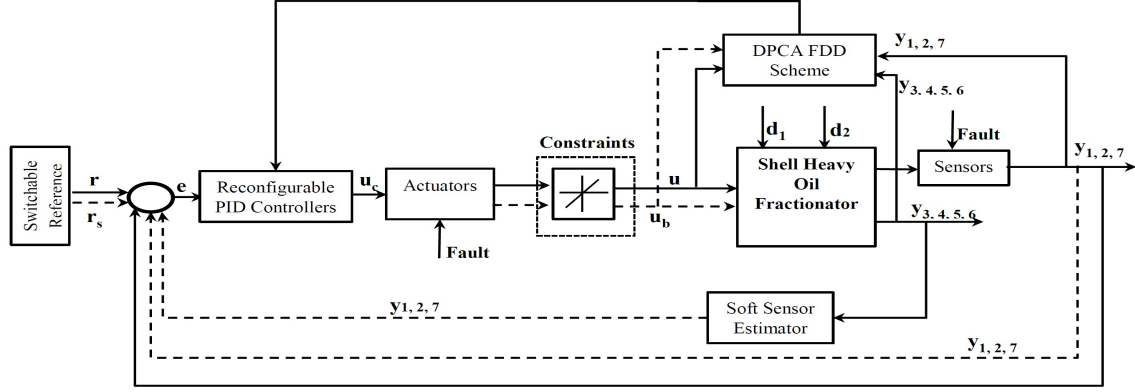
Fig. 10   Schematic of the Shell Heavy Oil Fractionator integrated with FTCS.

process operation. Gaussian noise of 0 mean and 0.003 standard deviation was added to each of the 7 outputs to represent true measurements of the data collected. Fig. 11 presents the system actuator outputs under normal operating conditions and their respective outputs responses to changes in set points and introduction of disturbances.
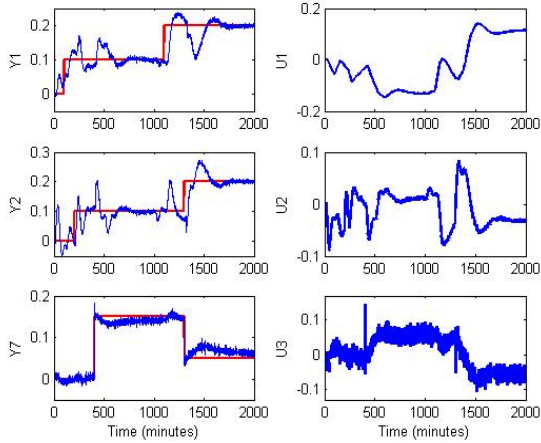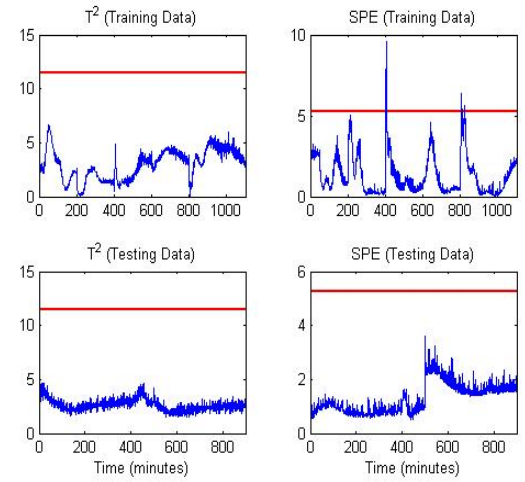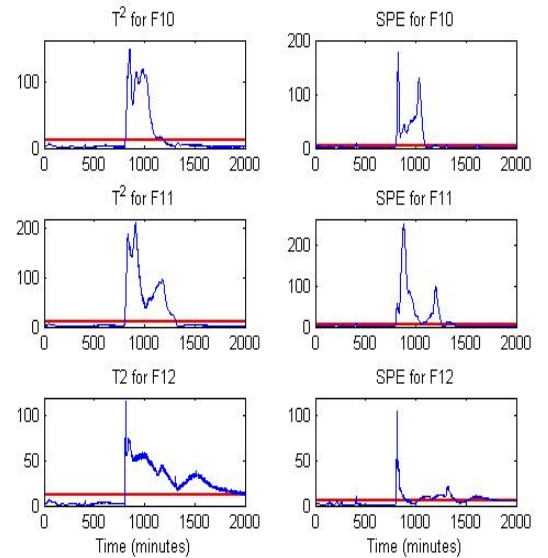

Fig. 11   Input and output responses to set point changes and disturbance rejection.

Table 5   Heavy oil fractionator fault list

Fault	Fault description
F10	Top draw actuator fault
F11	Side draw actuator fault
F12	Bottom reflux duty actuator fault

4.2   Faults introduction and detection

Three actuator faults (F10, F11 and F12) are investigated in this case as presented in Table 5, one each for the 3 actuators (u_1, u_2 and u_3). The fault was introduced in each case at 800 minutes as a constant value of 0.5 (i.e. control valve sticking to 0.5). The fault cases were each simulated for 2000 minutes to collect 2000 samples. Exactly the same procedure that was used to detect and diagnose actuator faults in the methanol-water separation column is

Fig. 12 T^2 and SPE monitoring performance for training and testing data

Fig. 13 T^2 and SPE monitoring performance for faults F10 – F12

applied here. 1100 samples of the 2000 samples collected during normal operating conditions were used to develop the DPCA diagnostic model while the remaining 900 samples were used for validation. The training data was scaled to zero mean and unit variance. Three principal components which account for 86.95% variation ($a = 3$) in the original data are used to develop DPCA model for process monitoring and actuator fault detection and diagnosis. Fig. 12 presents the process monitoring performance indices for the training and testing data sets.

The diagnostic model is applied to the three faulty actuator cases in the Shell heavy oil fractionator to detect possible fault occurrences. A fault is declared when the monitoring indices, T^2 and SPE violate their respective limits for 4 consecutive sampling times to ensure no false alarm is recorded. Fig. 13 presents the Hotelling's T^2 and SPE process monitoring performance for the 3 faults (F10 – F12). After a fault is declared, its root cause is further investigated through contribution plots which provide information on the contribution of each variable to the faulty scenario thereby aiding its isolation.

4.3 FTC implementation

When there is an actuator fault, the 3 by 3 control configuration used for normal process operation will have to be restructured, the reconfigurable controllers retuned

and the set points switched as appropriate upon detection and isolation of an actuator fault in order to maintain the integrity of the system. This is achieved through the backup feedback signals and set points as shown in Fig. 10. The different possible controller reconfigurations are assessed *a priori* using the RGA tool for the input-output pairings. When a fault is declared and identified, for instance top draw actuator fault (F10), we are left with just two healthy actuators, side draw and bottom reflux duty actuators (u_2 and u_3) to maintain three outputs at set points. This is practically impossible in the system being considered, therefore only two are controlled directly while the third is uncontrolled. We have chosen the top end and the side end points (y_1 and y_2) as the outputs to control during faulty operation by appropriately reconfiguring the remaining healthy actuators. An example of the RGA matrix obtained under F10 is given in (21) and Table 6 presents the inputs-outputs pairing for the three fault cases.

$$RGA_{F10} = \begin{bmatrix} -0.570 & 1.5702 \\ 1.5702 & -0.5702 \end{bmatrix} \qquad (21)$$

The error vector generated for the reconfigurable controller for the system during normal operation is obtained as (22) using (11). When the top draw actuator fault (F10) is declared and the fault tolerant controller reconfigures as appropriate, (23) is obtained.

$$e = \begin{bmatrix} 1 & 0 & 0 & 0 & 0 & 0 \\ 0 & 1 & 0 & 0 & 0 & 0 \\ 0 & 0 & 1 & 0 & 0 & 0 \\ 0 & 0 & 0 & 0 & 0 & 0 \\ 0 & 0 & 0 & 0 & 0 & 0 \\ 0 & 0 & 0 & 0 & 0 & 0 \end{bmatrix} \begin{bmatrix} r_1 \\ r_2 \\ r_2 \\ r_{s1} \\ r_{s2} \\ r_{s3} \end{bmatrix} - \begin{bmatrix} 1 & 0 & 0 & 0 & 0 & 0 \\ 0 & 1 & 0 & 0 & 0 & 0 \\ 0 & 0 & 1 & 0 & 0 & 0 \\ 0 & 0 & 0 & 0 & 0 & 0 \\ 0 & 0 & 0 & 0 & 0 & 0 \\ 0 & 0 & 0 & 0 & 0 & 0 \end{bmatrix} \begin{bmatrix} y_1 \\ y_2 \\ y_3 \\ y_{b1} \\ y_{b2} \\ y_{b3} \end{bmatrix} \qquad (22)$$

$$e = \begin{bmatrix} 0 & 0 & 0 & 0 & 0 & 0 \\ 0 & 0 & 0 & 0 & 0 & 0 \\ 0 & 0 & 0 & 0 & 0 & 0 \\ 0 & 0 & 0 & 1 & 0 & 0 \\ 0 & 0 & 0 & 0 & 1 & 0 \\ 0 & 0 & 0 & 0 & 0 & 0 \end{bmatrix} \begin{bmatrix} r_1 \\ r_2 \\ r_2 \\ r_{s1} \\ r_{s2} \\ r_{s3} \end{bmatrix} - \begin{bmatrix} 0 & 0 & 0 & 0 & 0 & 0 \\ 0 & 0 & 0 & 0 & 0 & 0 \\ 0 & 0 & 0 & 0 & 0 & 0 \\ 0 & 0 & 0 & 1 & 0 & 0 \\ 0 & 0 & 0 & 0 & 1 & 0 \\ 0 & 0 & 0 & 0 & 0 & 0 \end{bmatrix} \begin{bmatrix} y_1 \\ y_2 \\ y_3 \\ y_{b1} \\ y_{b2} \\ y_{b3} \end{bmatrix} \qquad (23)$$

Then, the fault tolerant control law under F10 is then given as:

$$u = \begin{bmatrix} u_1 \\ u_2 \\ u_3 \\ u_{b1} \\ u_{b2} \\ u_{b3} \end{bmatrix} = \begin{bmatrix} 0 \\ 0 \\ 0 \\ G_{b1} \\ G_{b2} \\ 0 \end{bmatrix} \begin{bmatrix} 0 \\ 0 \\ 0 \\ r_{s1} - y_{b1} \\ r_{s2} - y_{b2} \\ 0 \end{bmatrix} \qquad (24)$$

Table 6 Controlled and manipulated variables pairing

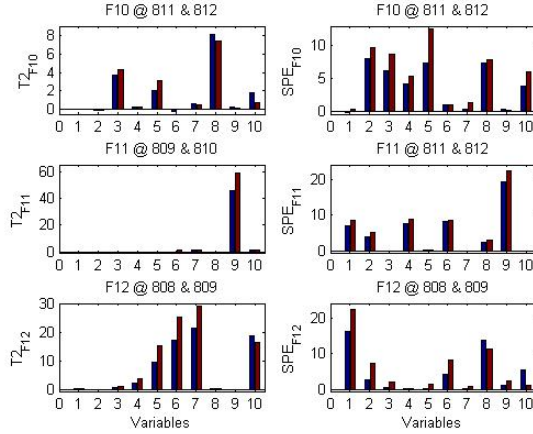| Controlled Outputs	Manipulated Inputs			
	Normal	F10	F11	F12
Top end point (y_1)	u_1	u_3	u_3	–
Side end point (y_2)	u_2	u_2	u_1	u_2
Bot. Reflux Temp. (y_7)	u_3	–	–	u_1

As shown in (23) and (24) above, the weightings for

different signals are activated or deactivated as appropriate to accommodate the fault declared and maintain the system within acceptable operating region.

4.4 Simulation Results

The three actuator faults investigated in this system – top draw actuator fault (F10), side draw actuator fault (F11) and the bottom reflux duty actuator faults (F12) were all detected. The DPCA diagnostic model monitoring statistics, T^2 and SPE detected the top draw actuator fault (F10) 11 minutes and 8 minutes respectively after its introduction as presented in Fig. 13. Side draw reflux actuator fault (F11) violated the T^2 and SPE monitoring limits at 809 and 807 minutes respectively while bottom reflux duty actuator fault (F12) was detected at 808 and 806 minutes respectively. Hotelling's T^2 and SPE variable contribution plots are analyzed at the point a fault is declared to investigate the root cause of the fault. The variable contribution plots shown in Fig. 14 presents excess

Table 7   Shell heavy oil fractionator reconfigurable PI controller settings

| Controlled Output Loop | Controller parameters | | | | | | | |
| | Normal | | F10 | | F11 | | F12 | |
	K_P	T_I	K_P	T_I	K_P	T_I	K_P	T_I
Top end point	0.05	0.0215	0.2	0.004	0.21	0.005	–	–
Side end point	0.45	0.0160	0.45	0.016	0.20	0.001	0.45	0.016
Bot. Reflux Temp.	3	0.005	–	–	–	–	1	0.020

Fig. 14 T^2 and SPE contribution plots for faults F10 – F12

contributions of each variable to the average values of T^2 and SPE that led to the fault being declared. Top temperature (variable 3) and top draw (variable 8) caused significant change in the correlation of the system variables which led to the fault, as identified by T^2 contribution plot. The SPE contribution plot shows side end point, top temperature, upper reflux temperature, side draw and bottom reflux duty (variables 2, 3, 4, 5, 8 and 10) as the major contributor to the faulty situation recorded. A critical analysis of the effect of top draw actuator fault (F10), depending on the magnitude of the fault shows a similar effect on the variables identified by the diagnostic model as being responsible for the fault. Though, the T^2 and SPE contribution plots give indications of likely causes of the fault, however an understanding of the system is still required to make the connections between the fault declared and the variables identified by the isolation technique.

The side draw actuator fault (F11) was caused by significantly large value of side draw (variable 9) which is the output of the faulty actuator as identified by contribution plots. SPE contribution plots in addition to the faulty actuator output also show top end point, side end point, upper reflux temperature and intermediate reflux temperature (variables 1, 2, 4, 6 and 9) as the variables responsible for the fault, as presented in Fig. 14. In the same vein, side draw temperature, intermediate reflux temperature, bottom reflux temperature and bottom reflux duty actuator output (variables 5, 6, 7, and 10) are identified by the T^2 contribution plots as the variables responsible for the bottom reflux duty actuator fault (F12). The SPE contribution plots indicate the top end point and the top draw actuator (variables 1 and 8) as the root cause of the fault. The pattern observed in this system for the bottom reflux duty actuator fault (F12) is similar to

the one observed in the steam valve actuator fault for the methanol-water separation column.

After the fault is detected and isolated as either being top draw actuator fault (u_1), side draw actuator fault (u_2) or bottom reflux duty actuator fault (u_3), it has to be accommodated so as to stabilize the system and ensure its continued operation, at least sub-optimally. When top draw actuator fault (u_1) occurs, clearly the 3 by 3 control structure will not be functional and depending on the severity of the fault, one of the remaining two healthy actuators, side draw actuator (u_2) and the bottom reflux duty actuator (u_3) are reconfigured to control the top end point (y_1). The input-output pairing used for FTC was discussed in the previous Section and presented in Table 6 while the reconfigurable PI controller settings for the system are presented in Table 7. Reflux duty actuator (u_3) is reconfigured to maintain the top end point at set point, leaving the bottom reflux temperature (y_7) uncontrolled, as shown in Fig. 15. The control structure reconfiguration was achieved through the backup feedback signals presented in Fig. 10. Appropriate backup feedback signals, in this case r_{s1} and y_{b1} were activated by changing their weightings from 0 to 1 and at the same time changing the weightings of the corresponding feedback signal to zero, as shown in (22). SP, NF, FR and AFR in Figs. 15 to 17 represent set points, no faults, fault responses and accommodated fault responses respectively. It can be observed from Fig. 15 that the bottom reflux duty was able to maintain the top end point at set point despite the influence of disturbances. Also, the performance of side end point control loop was slightly affected due to the strong interaction in the system.

In the case of side draw actuator fault (F11), none of the two remaining healthy actuators (u_1 and u_3) were able to accommodate the fault. Though the RGA analysis suggests the top draw (u_1) should be able to maintain the side end point (y_2) at set point, however its performance was very poor as can be observed from Fig. 16. The FTC was reconfigured to a 2 by 2 structure controlling the top end point (y_1) and side end point (y_2) by manipulating bottom reflux duty (u_3) and top draw (u_1) respectively making use of the backup feedback signals and reference point reconfiguration mechanism. Bottom reflux duty was able to keep the top end point at set point, however, top draw was not effective in maintaining side end point at set point. The bottom reflux temperature is uncontrolled having reduced the control configuration to 2 by 2.

The same scenario was observed when bottom reflux duty actuator fault (u_3) was declared. Neither of the two remaining healthy actuators, top and side draw actuators (u_1 and u_2) were able to control the bottom reflux temperature. Fig. 17 presents the fault tolerant controller
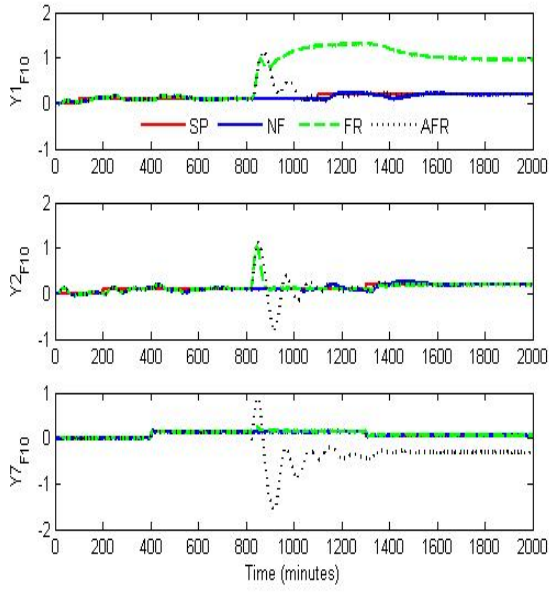
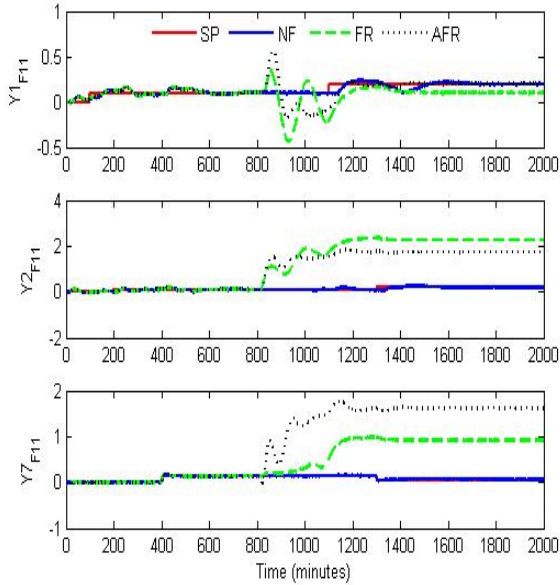Fig. 15   Output responses of accommodated actuator fault 10 (F10).

Fig. 16   Output responses of accommodated actuator fault 11 (F11).

performance for the bottom reflux duty actuator fault (F12) where top draw actuator (u_1) was reconfigured to control y_7. Observations from Fig. 17 show that implementation of fault tolerant controller in this particular case could not improve the system performance.

5   Conclusions

This work investigates the detection, identification and accommodation of actuator faults in distillation processes using comprehensive nonlinear simulation of a methanol-water separation column and the benchmark Shell heavy oil fractionator as examples. First, DPCA diagnostic model is developed from the data collected during normal process operation and is used for FDD. The DPCA effectively detects the faults and further diagnosis reveals the variables responsible for different faults through contribution analysis. When the detected fault is identified as an actuator fault, in the methanol-water separation column, one-point control strategy is implemented to directly control the more valued product composition leaving the other uncontrolled. The effect of disturbances on actuator fault propagation is also investigated. When the detected fault is identified as a composition sensor fault, then inferential control by-passing the faulty composition sensor needs to be implemented. This is under investigation and will be reported in the future. The effectiveness of the approach was demonstrated by the simulation results. Implementation of actuator fault tolerant controller is system dependent as different layers of performances have to be critically analyzed for the whole system and configured as backup in case such fault occurs. Actuator FTC is not always possible as observed in the case of the Shell heavy oil fractionator. Further application of the approach on a more complex system, for instance, a crude distillation unit with several actuator and sensor faults is currently being investigated.
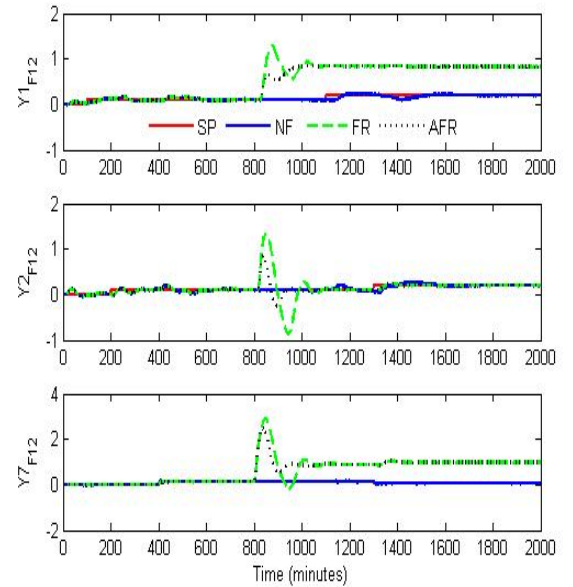

Fig. 17   Output responses of accommodated actuator fault 12 (F12).

Acknowledgement

Appendix

The complete transfer function model parameters for the Shell heavy oil fractionator are presented in Table A below.

Table A   Shell heavy oil fractionator transfer function model parameters

	Top draw (u₁)			Side draw (u₂)			Bot. reflux duty (u₃)			Int. reflux duty (d₁)			Upper reflux duty (d₂)		
	K	τ	θ	K	τ	θ	K	τ	θ	K	τ	θ	K	τ	θ
Top end point (y_1)	4.05	50	27	1.77	60	28	5.88	50	27	1.20	45	27	1.44	40	27
Side end point (y_2)	5.39	50	18	5.72	60	14	6.90	40	15	1.52	25	15	1.83	20	15
Top temperature (y_3)	3.66	9	2	1.65	30	20	5.53	40	2	1.16	11	0	1.27	6	0
Upper reflux temp. (y_4)	5.92	12	11	2.54	27	12	8.10	20	2	1.73	5	0	1.79	19	0
Side draw temp. (y_5)	4.13	8	5	2.38	19	7	6.23	10	2	1.31	2	0	1.26	22	0
Inter. reflux temp. (y_6)	4.06	13	8	4.18	33	4	6.53	9	1	1.19	19	0	1.17	24	0
Bottom reflux temp. (y_7)	4.38	33	20	4.42	44	22	7.20	19	0	1.14	27	0	1.26	32	0

References

[1] Bureau of Labor Statistics. Occupational injuries and illnesses in the United States by Industry. Washington, DC: Government Printing Office, 1998.

[2] McGraw-Hill Economics. Survey of investment in employee safety and health. NY: McGraw-Hill Publishing Co., 1985.

[3] National Safety Council. Injury facts 1999 Edition, Chicago: National Safety Council, 1999.

[4] V. Venkatasubramanian, R. Rengaswamy, K. Yin, and S. N. Kavuri. A Review of Process Fault Detection and Diagnosis. Part I. Quantitative Model-Based Methods, *Computers and Chemical Engineering*, 2003a, 27(3), 293–311.

[5] R. Isermann, Fault diagnosis of machines via parameter estimation and knowledge processing, - Tutorial paper. *Automatica*, 29(4), 815–835, 1993.

[6] V. Venkatasubramanian, R. Rengaswamy, and S. N. Kavuri. A Review of Process Fault Detection and Diagnosis. Part II. Qualitative Models and Search Strategies. *Computers and Chemical Engineering*. 2003b, 27(3), 313–326.

[7] R. C. Arkin and G. Vachtsefanos, Qualitative fault propagation in complex systems Proc. of the 29th IEEE CDC, Honolulu, HI, 1509-1510, 1990.

[8] V. Venkatasubramanian, R. Rengaswamy, R. Yin, and S. N. Kavuri. A Review of Process Fault Detection and Diagnosis. Part III. Process History Based Methods. *Computers and Chemical Engineering* 2003c, 27(3), 327–346.

[9] J. Zhang. Improved on-line process faults diagnosis through information fusion in multiple neural networks. *Computers and Chemical Engineering*. 2006, 30, 558–571.

[10] Y. Chetouani. Model selection and fault detection approach based on Bayes decision theory: Application to changes detection problem in a distillation column. *Process Safety and Environmental Protection* 92, 215–223, 2014.

[11] Y. Shu and J. Zhao. Fault diagnosis of chemical processes using artificial immune system with vaccine transplant. *Industrial and Engineering Chemistry Research* 55, 3360–3371, 2016.

[12] C. Zhao and W. Zhang. Reconstruction based fault diagnosis using concurrent phase partition and analysis of relative changes for multiphase batch processes with limited fault batches. *Chemometrics and Intelligent Laboratory Systems*. 130, 135–150, 2014.

[13] J. Yu, J. Chen and M. M. Rashid. Multiway independent component analysis mixture model and mutual information based fault detection and diagnosis approach of multiphase batch processes. *American Institute of Chemical Engineers Journal*. 59 (8), 2761–2779, 2013.

[14] F. Harrou, M. N. Nounou, H. N. Nounou and M. Madakyaru. PLS-based EWMA fault detection strategy for process monitoring. *Journal of Loss Prevention in the Process Industries*. 36, 108–119, 2015.

[15] Y. Zhang and J. Jiang. Bibliographical Review on Reconfigurable Fault Tolerant Control Systems. *Annual Review in Control* 32, pp. 229–252, 2008.

[16] D. Chilin, J. Liu, D. Munoz de la Peria, P. D. Chritofides and J. F. Davis. Detection, isolation and handling of actuator faults in distributed model predictive control systems. *Journal of Process Control* 20, 1059–1075, 2010a.

[17] D. Chilin, J. Liu, J. F. Davis, and P. D. Christofides. Data-based monitoring and reconfiguration of a distributed model predictive control system. *International Journal of Robust and Nonlinear Control* 22, 68–88, 2012.

[18] A. Mirzaee and K. Salahshoor. Fault diagnosis and accommodation of nonlinear systems based on multiple-model adaptive unscented Kalman filter and switched MPC and H-infinity loop-shaping controller. *Journal of Process Control*. 22, 626–634, 2012.

[19] L. Lao, M. Ellis and P. D. Christofides. Proactive Fault-Tolerant Model Predictive Control. *American Institute of Chemical Engineers Journal* Vol. 59, No. 8, 2810–2820, 2013.

[20] J. MacGregor and A. Cinar. Monitoring, fault diagnosis, fault-tolerant control and optimization: Data driven methods. *Computer and Chemical Engineering* 47(2012), 111–120, 2012.

[21] J. Love. *Process automation handbook: a guide to theory and practice.* Springer-Verlag, London, pp. 243–260, 2007.

[22] T. E. Marlin. *Process control: designing processes and control systems for dynamic performance.* 2nd ed., McGraw Hill, 2000.

[23] W. L. Luyben. *Practical distillation control.* Van Nostrand, 1992.

[24] P. B. Deshpande. *Distillation dynamics and control.* ISA, Carolina, 1985.

[25] J. Zhang and R. Agustriyanto. Multivariate inferential feed-forward control. *Industrial and Engineering Chemistry Research* 2003, 42, 4186–4197.

[26] M. T. Tham, F. Vagi, A. J. Morris and R. K. Wood. [Online] Multivariable Adaptive Control of a Binary Distillation Column. *Canadian Journal of Chemical Engineering*. 69, 997–1009, 1991.

[27] M. T. Tham, F. Vagi, A. J. Morris and R. K. Wood. Multivariable and Multirate Self-Tuning Controls A Distillation Column Case Study. *IEE Proceedings Pt. D, Control Theory Applications*. 138, 9–24, 1991.

[28] S. A. Lawal and J. Zhang. Actuator fault monitoring and fault tolerant control in distillation columns. *Proceedings of the 21st International Conference on Automation and Computing (ICAC2015)*. Glasgow, pp. 329–334, Sept. 11–12, 2015.

[29] D. M. Prett and M. Morari. *The Shell process control workshop.* London, Butterworths, 1987.

[30] C. Vlachos, D. Williams and J. B. Gomm. Solution to the Shell standard control problem using genetically tuned PID controllers. *Control Engineering Practice* 10, 151–163, 2002.

Jie Zhang received his BSc degree in Control Engineering from Hebei University of Technology, Tianjin, China, in 1986 and his PhD degree in Control Engineering from City University, London, in 1991. He is a Lecturer in the School of Chemical Engineering and Advanced Materials, University of Newcastle, England.

His research interests are in the general areas of process system engineering including process modelling, batch process control, process monitoring, and computational intelligence. He has published over 250 papers in international journals, books, and conferences. He is a Senior Member of IEEE, a member of the IEEE Control Systems Society, and IEEE Computational Intelligence Society. He is on the Editorial Boards of a number of journals including Neurocomputing published by Elsevier.

E-mail: jie.zhang@newcastle.ac.uk

Sulaiman Ayobami Lawal received his BSc. degree in Chemical Engineering from Ladoke Akintola University of Technology, Nigeria in 2003 and M.Sc. in Applied Process Control from Newcastle University, UK in 2006. He is a lecturer at the Chemical Engineering Department of the University of Lagos, Akoka, Yaba in Nigeria and currently a PhD candidate at Newcastle University, UK.

His research interest is on actuator and sensor fault detection and diagnosis and fault tolerant control systems.

E-mail: s.a.lawal@newcastle.ac.uk (Corresponding author)
ORCID iD:0000-0002-0485-9141